JOS

Lab #3

Josephson Junction

Alison Y. Kim
SID 23780367

Partner:
Saavanth Velury
SID 23584407

Instructors:
Prof. H. Haeffner
Prof. K.B. Luk

Physics 111B
Spring 2016

Due 13 April 2016

1 Abstract

This experiment aims to introduce the theoretical and experimental workings of the Josephson effect. Lessons of electrodynamics, quantum mechanics, and solid state physics were supplemented with laboratory techniques and data analysis. To this end, my partner and I built our own Josephson junction using a niobium (Nb) wire and screw as superconductors, separated by a thin, insulating oxide layer on the surface of the wire point. The junction was mounted onto a probe and subsequently lowered into a cryostat filled with liquid helium (He), an ultracold ($T = 4$ K) environment conducive to superconductivity. Finally, we confirmed the presence of DC and AC Josephson effects by using a four-wire impedance measurement to empirically compute the Josephson constant, $\frac{2e}{h}$, which we found to be 476.0 ± 56 MHz/μV. The objectives of this report are (1) to explain the phenomena that give rise to superconductivity, (2) to summarize and justify the undertaken procedures, and (3) to analyze the recorded data and account for any uncertainties in our measurements.

2 Introduction

The Josephson junction is rightly celebrated as one of the most significant 20^{th} century contributions to physics and engineering. It consists of two **superconductors** weakly coupled by an insulating layer. In 1962 Brian D. Josephson theorized that if a steady potential V is maintained across the two superconductors, a supercurrent will flow between them at a frequency $\nu = \frac{2e}{h}V$ [1]. This theory was verified experimentally by Philip Anderson and John Rowell in 1973, and has since been reproduced countless times in research and classroom settings.

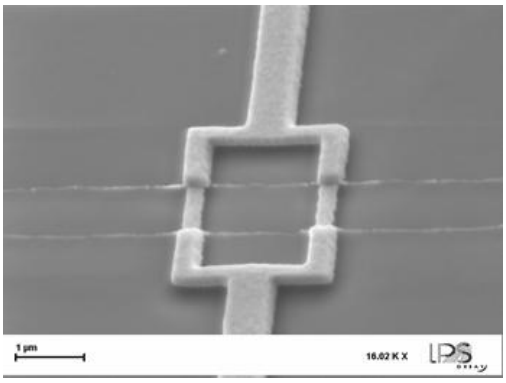

Figure 1: A **s**uperconducting **qu**antum **i**nterference **d**evice, or SQUID, is used to precisely measure subtle magnetic fields. Such magnetometers consist of superconducting loops, shown above, that contain Josephson junctions. Image sourced from [2].

Unbeknownst to physicists at the time, supercurrents had been observed in superconductors prior to 1962, but they were believed to have resulted from unintentional punctures in the insulating layer, which would provide a means for direct electron conduction between the superconductors [3]. Additionally, it had been known that "normal" (that is, non-superconducting) electrons could breach an insulating layer via **quantum tunneling**, but it was not until Josephson's prediction of *superconducting* electrons bound as Cooper pairs that a more comprehensive model was proposed. It is this model that crowned him a Nobel laureate in 1973, and he has remained an important figure in the field of condensed matter physics.

The educational significance of Josephson's discovery lies in its bridging microscopic quantum phenomena with macroscopic, everyday experiences. Its applications have broadened the field of digital electronics, the most famous of which is the magnetic field-detecting SQUID (see Figure 1). It has also allowed for increasingly precise measurements of fundamental constants; for instance, our experiment uses a current source, voltmeter, and bar magnet—all common laboratory apparatuses—along with small quantities of superconducting material in order to measure $\frac{2e}{h}$. Despite the difficulties involved in constructing sensitive devices, maintaining secure electronic connections, and taking careful measurements, the Josephson junction experiment is of great importance to a student of physics as it sheds insight into the quantum world. Not to mention, it serves as a practical means of reinforcing important concepts from quantum mechanics and electrodynamics.

To carry out the experiment, my partner and I first constructed a Josephson junction using a Nb needle and screw as the superconducting boundaries, separated by an insulator in the form of oxide that accumulated on the surface of the needle. We carefully mounted the junction onto a probe, which served to hold the junction in place and connect it to the current source and oscilloscope. After using a multimeter to ensure each electrical connection, we lowered the probe into a liquid He cryostat, the purpose of which was to create a low-temperature environment in which Cooper pairs could form and flow as a supercurrent. This setup allowed us to observe the Josephson effect on the oscilloscope and estimate the fundamental constant of interest: $\frac{2e}{h}$. In the following sections, I shall expound the elegant theory of the Josephson effect and present supporting experimental evidence, complete with procedural details and error analysis.

3 Theory

A **Josephson junction** is made of two superconductors weakly linked by an insulating (or any other non-superconducting) layer. The insulator functions as an electrical barrier through which electrons must tunnel. While an introductory quantum mechanics course provides a description of this tunneling for "normal", non-superconducting electrons, a slightly different approach must be taken to analyze the behavior of superconducting electrons.

3.1 Definitions & Preliminary Calculations

Superconductivity describes the phenomena of zero electrical resistance and expulsion of magnetic fields that occur in certain materials. Below a critical temperature, a conductor will transition into the superconducting state, during which magnetic field lines are expelled from the interior of the material, a process called the Meissner effect. A concomitant result is the formation of quasi-bosonic **Cooper pairs** between free *fermionic* electrons, as the repulsive Coulomb forces are overcome by the attractive electron-phonon interactions. Such pairs do not obey the Pauli exclusion principle, which prevents two electrons from occupying the same quantum state. As a result, Cooper pairs can condense to the same low-energy quantum states well below the Fermi energy.

The electrons in a Cooper pair need not be physically close to each other because electron-phonon interaction is long range [4]. Instead, the efficiency of Cooper pairing depends most strongly on a pair's phase coherence throughout the superconductor. Since superconductivity is quantum mechanical, the electrons in a particular superconducting state can collectively be described by a time-dependent wavefunction (see Figure 2). Then, the associated wavefunctions of electrons in

two separate superconducting regions are

$$\begin{aligned}\Psi_1(r,t) &= |\Psi_1(r,t)|\, e^{i\phi_1(r,t)} \\ \Psi_2(r,t) &= |\Psi_2(r,t)|\, e^{i\phi_2(r,t)}\end{aligned} \tag{1}$$

where ϕ_i denote the respective phases as functions of position r and time t. In a Josephson junction, the condition of phase coherence means that the phase of one state must be related to the phase of the second by some additive factor $\Delta\phi$. Then (1) becomes

$$\begin{aligned}\Psi_1(r,t) &= |\Psi_1(r,t)|\, e^{i\phi_1(r,t)} \\ \Psi_2(r,t) &= |\Psi_2(r,t)|\, e^{i[\phi_1(r,t)+\Delta\phi]}\end{aligned} \tag{2}$$

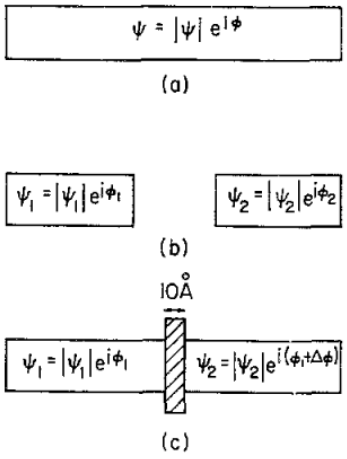

Figure 2: A graphical depiction of assigning a wavefunction to (a) any superconductor, (b) two isolated superconductors, and (c) two superconductors coupled by a weak link, as in a Josephson junction. Image sourced from [1].

Let us temporarily drop the functional notation (r,t) for simplicity. Assuming the junction is symmetrical (this is a valid assumption if both superconductors are made of the same material, as is the case in this experiment), the wavefunctions are related by

$$\begin{aligned}i\hbar\frac{\partial\Psi_1}{\partial t} &= U_1\Psi_1 + K\Psi_2 \\ i\hbar\frac{\partial\Psi_2}{\partial t} &= U_2\Psi_2 + K\Psi_1\end{aligned} \tag{3}$$

where K is a coupling characteristic and U_i are the lowest energies of each superconducting region [5]. Let V be the potential difference across the junction. Then $U_1 - U_2 = qV$, where q is the charge of the Cooper pair. Following Feynman's convention, define the zero of energy to occur at the midpoint between the superconductors' lowest energies, $\frac{qV}{2}$. Then (3) becomes

$$\begin{aligned}i\hbar\frac{\partial\Psi_1}{\partial t} &= +\frac{qV}{2}\Psi_1 + K\Psi_2 \\ i\hbar\frac{\partial\Psi_2}{\partial t} &= -\frac{qV}{2}\Psi_2 + K\Psi_1\end{aligned} \tag{4}$$

3.2 Josephson Effect

When studying any electrical device, one property of interest is the current-voltage relationship, or the I-V characteristic. Thus, it is convenient to interpret the above wavefunctions in terms of

electron densities $\rho_i(r,t)$. Define $\rho_i(r,t) \equiv |\Psi_i(r,t)|^2$. Then (2) becomes

$$\begin{aligned} \Psi_1(r,t) &= \sqrt{\rho_1(r,t)}e^{i\phi_1(r,t)} \\ \Psi_2(r,t) &= \sqrt{\rho_2(r,t)}e^{i[\phi_1(r,t)+\Delta\phi]} \end{aligned} \tag{5}$$

Each wavefunction now has two time-dependent variables, and substitution of (5) into (3) subsequently yields expressions for the changes in charge density and phase over time. The first quantity represents the **supercurrent** flowing through the junction and is given by

$$I(t) = I_0 \sin[\Delta\phi(t)] \tag{6}$$

where I_0 is the maximum allowed zero-voltage current [1]. Because this supercurrent occurs in a Josephson junction, the phenomenon is aptly named the **Josephson effect**.

The second quantity is the rate of change of phase difference across the junction [5]:

$$\begin{aligned} \frac{\partial\Delta\phi}{\partial t} &= \frac{\partial\Delta\phi}{\partial t} \\ &= \frac{\partial\phi_2}{\partial t} - \frac{\partial\phi_1}{\partial t} \\ &= \frac{q}{\hbar}V(t) \end{aligned} \tag{7}$$

Since two electrons comprise a Cooper pair, $q = 2e$ and (7) can be written as

$$\frac{\partial\Delta\phi}{\partial t} = \frac{2e}{\hbar}V(t) \tag{8}$$

The Josephson constant $\frac{2e}{\hbar}$ mentioned in **Section 2** is thus the proportionality constant between the change in phase difference and the potential across the junction.

Integrating (8) yields an expression for the phase difference,

$$\Delta\phi(t) = \frac{2e}{\hbar}tV(t) + \Delta\phi_0 \tag{9}$$

where $\Delta\phi_0$ is the constant of integration. Depending on the nature of $V(t)$, the explicit expressions for $I(t)$ and $\Delta\phi(t)$ will differ.

3.2.1 DC Josephson Effect

Let $V(t)$ be a DC voltage V_{DC} applied across the junction. Then (9) becomes

$$\Delta\phi(t) = \frac{2e}{\hbar}tV_{DC} + \Delta\phi_0 \tag{10}$$

and the supercurrent equation is simply

$$I(t) = I_0 \sin\left(\frac{2e}{\hbar}tV_{DC} + \Delta\phi_0\right) \tag{11}$$

The supercurrent ranges from $[-I_0, +I_0]$ when the sine term yields ∓ 1, respectively. This is known as the **DC Josephson effect**. Clearly, Cooper pairs can quantum mechanically tunnel even in the absence of an external electromagnetic field.

3.2.2 AC Josephson Effect

Now suppose we apply an external field in the form of an AC voltage with a DC bias, expressed as $V(t) = V_{DC} + V_{AC}\cos(\omega t)$. Due to the time-dependent voltage term, we must derive the phase difference explicitly by plugging $V(t)$ into (8) to obtain

$$\begin{aligned}\Delta\phi(t) &= \frac{2e}{\hbar}\int dt[V_{DC} + V_{AC}\cos(\omega t)] \\ &= \frac{2e}{\hbar}[V_{DC}t + \frac{V_{AC}}{\omega}\sin(\omega t)] + \Delta\phi_0\end{aligned} \tag{12}$$

and now (12) into (6) for the supercurrent equation

$$I(t) = I_0 \sin\{\frac{2e}{\hbar}[V_{DC}t + \frac{V_{AC}}{\omega}\sin(\omega t)] + \Delta\phi_0\} \tag{13}$$

Following Feynman's method [5], we can assume that the argument of the sine term is small, in which case the approximation $\sin(x + \Delta x) \approx \sin(x) + \Delta x\cos(x)$ is valid. Then we may rewrite (13) as

$$I(t) \approx I_0[\sin(\frac{2e}{\hbar}V_{DC}t + \Delta\phi_0) + \sin(\omega t)\cos(\frac{2e}{\hbar}V_{DC}t + \Delta\phi_0)] \tag{14}$$

The first sine term usually approaches zero since its argument is highly oscillatory, but when $\omega = \frac{2e}{\hbar}V_{DC}$, the second term survives. Define $\omega t \equiv \Delta\phi$ and the magnetic flux $\Phi \equiv V_{DC}t$. Then (14) simplifies to

$$I(t) \approx I_0 \sin(\Delta\phi)\cos(\frac{2e}{\hbar}\Phi) \tag{15}$$

Since the maximum value of $\sin(\Delta\phi)$ is 1, the maximum current is

$$I_{max} = I_0\cos(\frac{2e}{\hbar}\Phi) \tag{16}$$

which itself reaches extrema whenever $\Phi = n\frac{\pi\hbar}{2e}$ for some nonnegative integer n. (Magnetic flux is indeed quantized!) Recalling the definition of Φ and letting ω represent an arbitrary angular frequency, we observe that

$$\frac{2e}{\hbar} = \frac{n\omega}{V_{DC}} \tag{17}$$

is the condition under which the **AC Josephson effect** will occur.

4 Procedure

4.1 Apparatus

This experiment uses a point-contact junction (see Figure 3a). The superconductors are made of niobium (Nb), a transition metal that exhibits superconducting properties below the critical temperature $T = 9.2$ K [6]. Any surface in contact with air will oxidize to form niobium-oxide, which serves as the insulating layer. For niobium to achieve superconductivity and aid the formation of Cooper pairs, the junction was mounted onto a cryo-probe (see Figure 3b) and lowered into a dewar containing ultracold liquid He, which exists in this phase at $T = 4$ K.

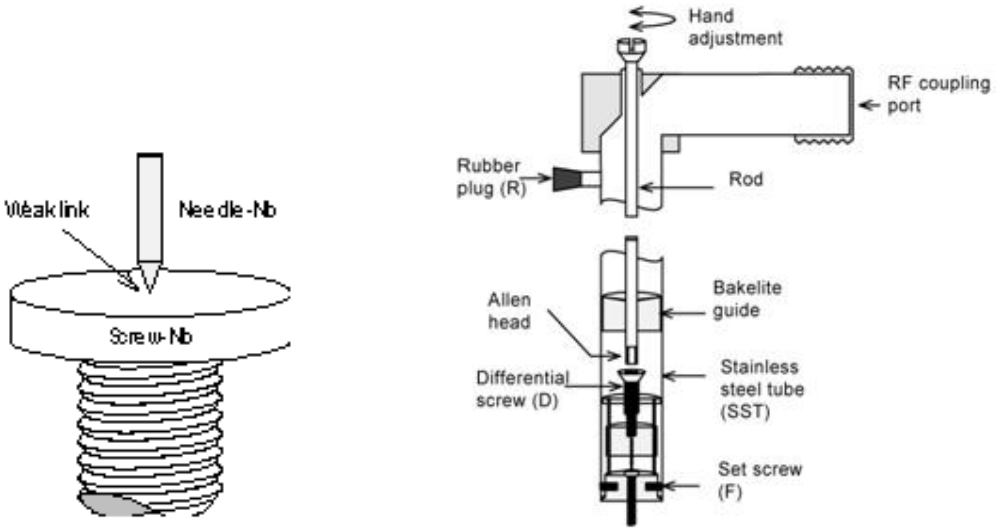

(a) Josephson point-contact junction: Needle-Nb and Screw-Nb are the superconducting regions that are coupled by the weak link of oxide.

(b) Josephson junction contacts: Needle-Nb and Screw-Nb are the superconducting regions that are coupled by the weak link of oxide.

Figure 3: Images sourced from [7].

The second function of the cryo-probe is to provide a means of measuring the electrical resistance of the junction. Since this value is very small in a superconducting state, we used a four-wire setup (see Figure 4) to ensure that the internal series-lead impedances intrinsic to the physical probe would be corrected for when measuring the junction resistance [8].

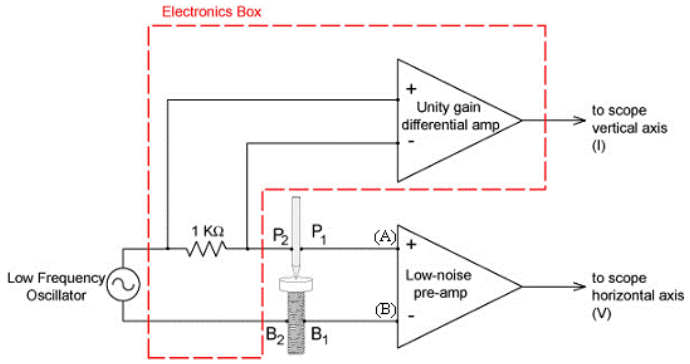

Figure 4: The four-wire measurement mapped out in terms of electrical connections. A current was applied at probe outputs B2 and P2, and the voltage drop was measured using outputs B1 and P1. Image sourced from [7].

4.2 Building the Josephson Junction

One of the two superconductors was constructed using a short Nb wire, one end of which was filed into a conical point (see Figure 5a). To facilitate the oxidation process and ensure a stable insulating layer, we smoothed the tip surface with fine sandpaper and left the needle in a Petri dish over the course of a weekend. To make the contact, we inserted the needle into the junction assembly into which the other superconductor was already inserted (see Figure 5b). The assembly was secured with a differential screw and mounted onto the probe.

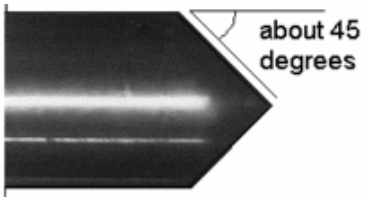

(a) The desired conical shape of the needle tip, formed by filing one end of Needle-Nb. Oxidation will turn the surface a brown-reddish color.

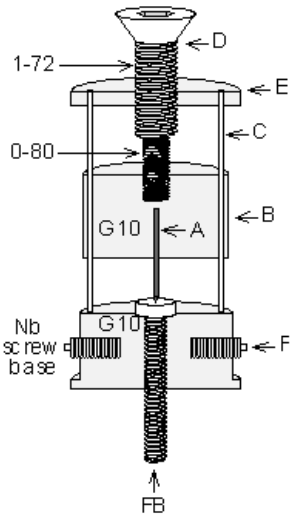

(b) Junction assembly.

Figure 5: Images sourced from [7].

4.3 Electrical Connections

To confirm that no unintentional electrical connections had been made while integrating the junction into the probe, we checked that an infinite resistance separated each output (B1, B2, P1, P2) from (1) a neighboring output and (2) the metal body of the probe (ground). Then, we connected a digital ohmmeter to B1 and P1 and tightened the hand adjustment until the resistance changed from `OVERLOAD` (i.e., infinite) to approximately a few ohms. A closed non-superconducting circuit should allow current flow, and thus a nontrivial resistance measurement.

Finally, we generated a driving signal of $f = 60$ Hz and $Amp = 4$ V and tuned a low-noise pre-amplifier with a bandwidth $b \in [0.03, 30 * 10^3]$ Hz and gain $A \in [5 * 10^2, 2 * 10^3]$. (We tuned the gain during the AC effect portion of the experiment.) Once the probe outputs were properly connected to the signal generator and oscilloscope, we confirmed our expectation of a linear I-V curve (see Figure 6), whose inverse slope represented the internal resistance of the oscilloscope.

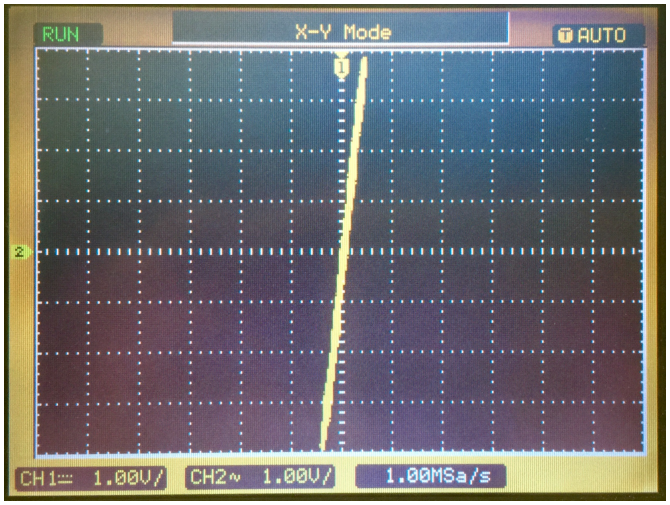

Figure 6: I-V curve just after all of the electrical connections have been made from the probe to the current source, pre-amplifier, and oscilloscope. The horizontal axis represents voltage on the scale of `1.00 V/div`, and the vertical axis represents current on the scale of `1.00 A/div`. Image captured using iPhone 6S Plus.

To assess the reliability of our measurements, we checked whether the room-temperature internal resistance of the scope was within error of a reading provided by a digital multimeter (DMM). Estimating an error of 10% from simply reading off values, the oscilloscope calculation (see Figure 6 caption for division scale) yielded

$$\begin{aligned} R_{scope} &= \frac{V}{I} = \text{slope}^{-1} \\ &= \frac{0.45\ \text{V} - 0\ \text{V}}{3.9\ \text{A} - 0\ \text{A}} \\ &\approx 0.12 \pm 0.012\ \Omega \end{aligned}$$

For the DMM reading, we used the four-wire resistance measurement and noted a 2% calibration error from the `Hewlett-Packard 3465A Multimeter` manual provided at the JOS station. Probing the resistance between P1 and B1, the resistance of the scope was found to be

$$R_{DMM} \approx 0.132 \pm 0.00264\ \Omega$$

The two measurements are indeed within error of each other.

Additionally, it is important to match the driving frequency of the signal generator to the frequency of the background noise—that is, the all-too-familiar 60 Hz intrinsic to all real-life electronic devices. Otherwise, the scope may display a signal that has picked up attenuated portions of background noise and thus degrade our measurements. Since the signal in Figure 6 was linear and not noisy, we assumed that the frequencies were successfully matched.

4.4 Observing the DC Effect

After lowering the probe into the dewar, we adjusted the junction pressure by slowly twisting the screw. We also made sure to adjust the gain so that the effect could be clearly observed without overloading the pre-amplifier; we found that the appropriate gain was $1 * 10^3$. These parameters were varied until the oscilloscope display changed from the line shown in Figure 6 to the curve shown in Figure 7. To ensure that this was truly the DC effect in action, we brought a large magnet near the dewar and observed fluctuations in the I-V curve.

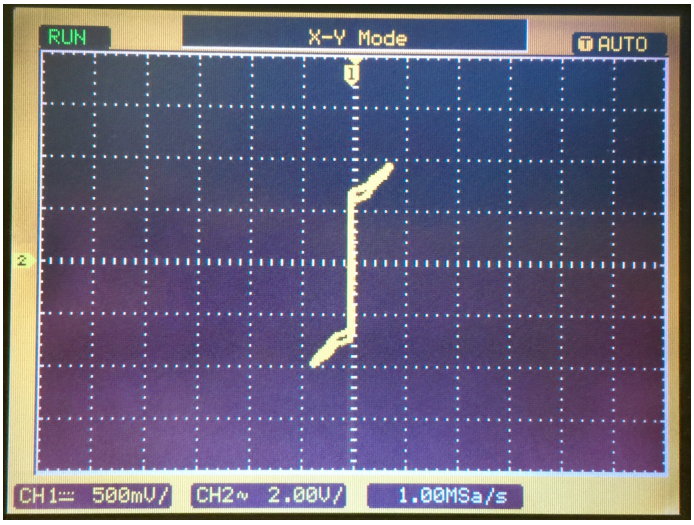

Figure 7: The DC Josephson effect. Vertical scale is `0.500 mA/div`, and horizontal scale is `2.00 V/div`. See **Section 5.1** for a recreated I-V plot, which uses actual data points extracted with the `Josephson junction.vi` program made available by the 111B lab. Image captured using iPhone 6S Plus.

4.5 Observing the AC Effect

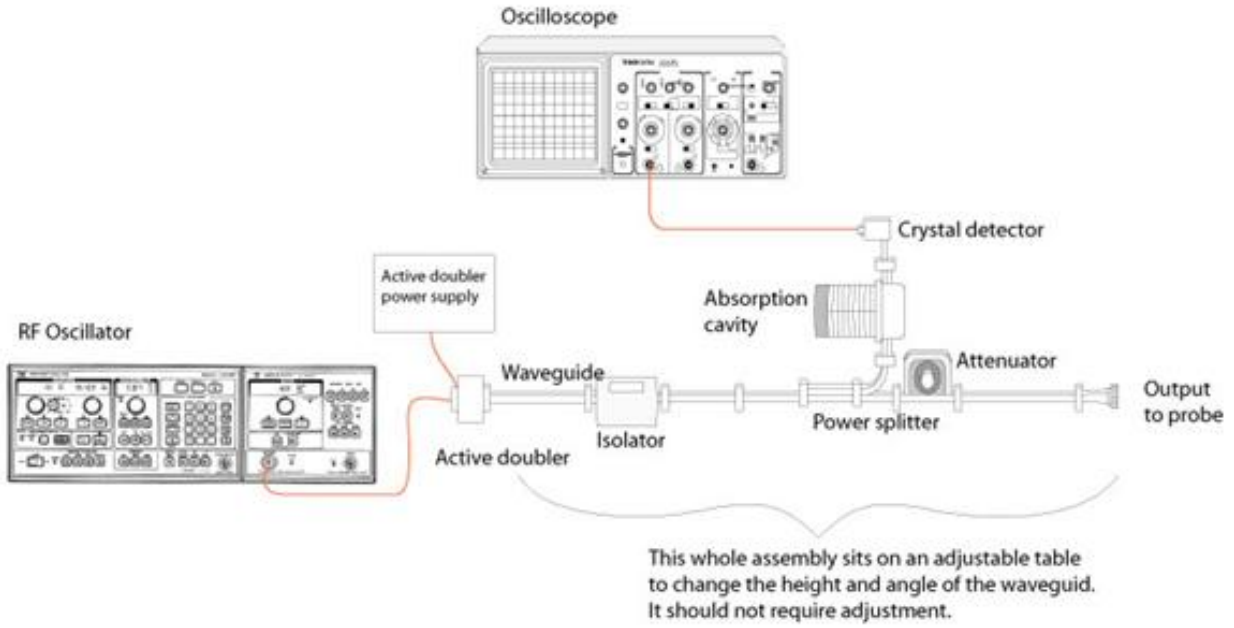

Figure 8: Relevant equipment for the AC effect portion of the experiment. Image sourced from [7].

Once the DC effect was observed, we applied an external electromagnetic field to the junction in the form of microwaves, which were generated by the radio frequency (RF) oscillator. The waves doubled in frequency through the active doubler, then traveled through the waveguide before being split into separate trajectories. One led the microwaves to the absorption cavity and crystal detector, which allowed us to measure the microwave frequency quite precisely. The other trajectory led the microwaves through a power attenuator and finally to the output to the probe, where the radiation could finally reach the junction. Figure 8 gives a graphical depiction of the process.

To optimize the AC effect, we adjusted a combination of three different parameters: RF frequency ($f_{RF} \in [9, 13]$ GHz), RF power (attenuation $\in [0, 20]$ dB), and junction pressure (manually adjustable screw). First, we increased the pressure until we could just feel the tip of the hand adjustment mating with the differential screw (see Figure 3b); adding pressure beyond this point runs the risk of scraping off the insulating layer from the needle surface. Starting with maximum attenuation of 20 dB (i.e., lowest power), we slowly scanned the suggested frequency range; using a smaller step (on the order of, say, 100 MHz) would result in achieving the critical current *before* seeing any signs of an AC effect. After several days of scanning other values of attenuation and adjusting the pre-amplifier gain, we found a working AC effect at a frequency of $f_{RF} = 9.5204$ GHz, attenuation of 20 dB, and gain of 2 (see Figure 9). The frequency reading from the crystal detector showed that the RF frequency was actually $f_{CD} = 19.130$ GHz. The error from the frequency readings will be discussed in **Section 5.2**.

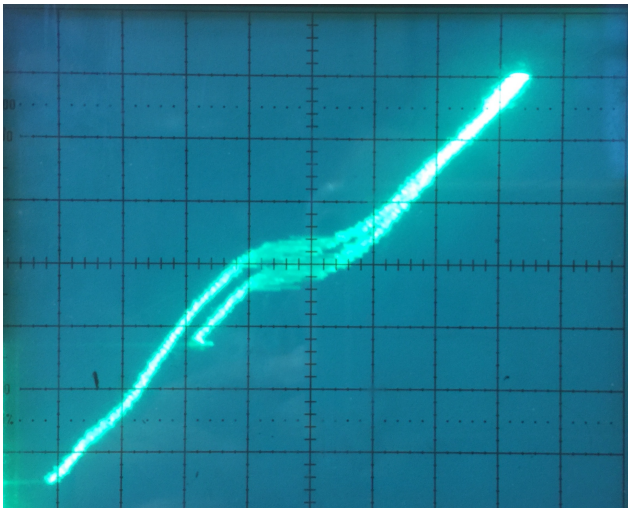

Figure 9: The AC Josephson effect. Vertical scale is `0.500 mA/div`, and horizontal scale is `0.500 V/div`. The scope photo captured the general shape of the desired curve, but the steps were hidden within the flatter region of the curve. See **Section 5.2** for a recreated I-V plot, which uses actual data points extracted with the `Josephson junction.vi` program made available by the 111B lab. Image captured using iPhone 6S Plus.

4.6 Calibration

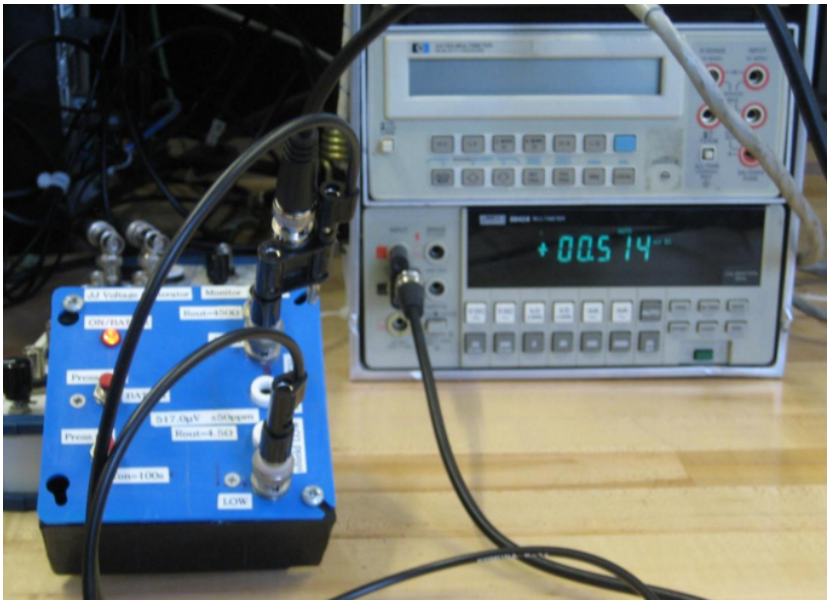

Figure 10: Voltage box used to measure the signal's end-to-end gain. Image sourced from [7].

In order to make accurate calculations of $\frac{2e}{h}$, it was important to optimize the bandwidth of the voltage axis more so than the current axis. This is because the voltage values are directly used in computing the Josephson junction whereas the current values are not. To this end, we used the end-to-end gain technique as a means of calibration. First, we connected a voltage box to the DMM and measured its voltage to be $V_{box} = 0.514 \pm 0.0103$ mV. Then, we connected the box to the oscilloscope and measured the RMS amplitude of the box signal received by the pre-amplifier to be $V_{sig} = 0.0031 \pm 0.000062$ V $= 3.1 \pm 0.062$ mV. The resulting end-to-end gain was obtained by dividing the RMS voltage by the box voltage, yielding 6.031 ± 0.654. We used this result to calibrate the voltage axes by dividing the raw voltage data values by this value.

5 Analysis

5.1 DC Effect

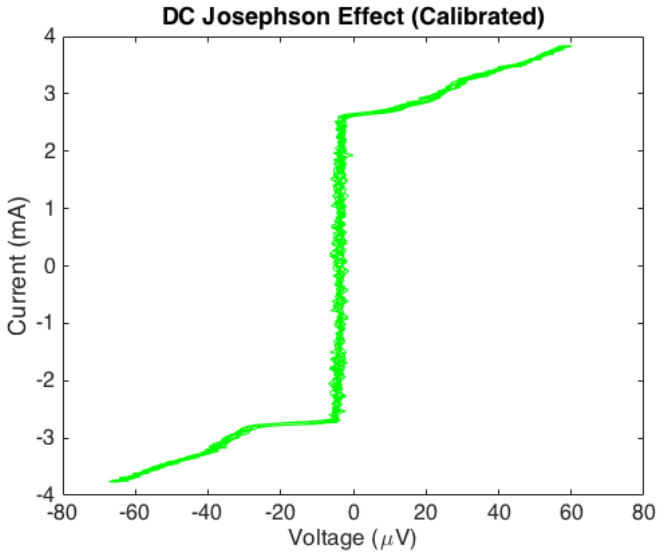

Figure 11: Voltage-calibrated plot of the DC effect I-V characteristic. Data taken using the `Josephson junction.vi` program provided by the 111B lab. Plot generated in `MATLAB`.

Figure 11 shows the recreated plot of the DC effect data. The discontinuity occurs along the range of current values between $\mp I_{crit}$ and represents the tunneling region. While we expected it to occur exactly at $V = 0$ V, there is a slight leftward offset of about 4 μV, which likely resulted from the internal series resistance of the cryo-probe.

5.2 AC Effect & Calculation of $\frac{2e}{h}$

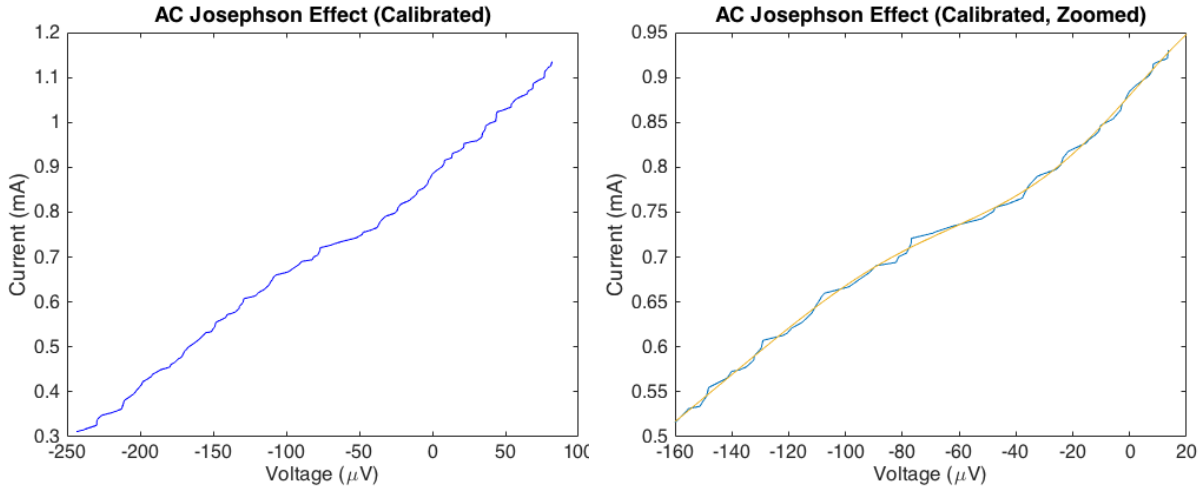

(a) Voltage-calibrated plot of the AC effect I-V characteristic. Data taken using the `Josephson junction.vi` program provided by the 111B lab.

(b) Voltage-calibrated plot, zoomed in on the "step" and fitted with `CurveFit.m` script provided by the 111B lab.

Figure 12: Plots generated in `MATLAB`.

Figure 12a shows the recreated plot of the AC effect data. As mentioned in **Section 4.6**, the microwave frequency was set to $f_{RF} = 9.5204$ GHz but was measured to be $f_{CD} = 19.130$ GHz after undergoing doubling. The attenuation of 20 dB proved sufficient in producing the AC effect. While only one step was produced, it was enough to calculate the Josephson constant.

Recall the condition for the AC effect that is given by (17). With $n = 1$ and converting $\hbar$ and ω to their linear analogues h and f, respectively, (17) can be rewritten as

$$K_J = \frac{2e}{h} = \frac{f}{V} \tag{18}$$

where f indicates the microwave frequency and V is the voltage step size. In order to characterize the voltage step and calculate V, I zoomed in on the data (see Figure 12b) and determined that the two inflection points marked the beginning and end of the step that we observed. To extract these points, I used the `CurveFit.m` script, which determined a fit with a reduced chi-square value of $\chi^2/df = 0.964$, and found that the inflections occur at -80 ± 0.8 μV and -40 ± 0.4 μV. Taking their absolute difference, the step size is $V = 40 \pm 0.4$ μV. Then, I divided this voltage step by the pre-amplifier gain $A = 2$ to obtain $V = 20 \pm 0.2$ μV. Plugging this value along with $f = 9.5204$ GHz into (17) yields

$$\begin{aligned} \frac{2e}{h} = K_J &= \frac{f}{V} \\ &= \frac{9.5204 \text{ GHz}}{20 \ \mu\text{V}} \\ &\approx 476.0 \text{ MHz}/\mu\text{V} \end{aligned}$$

Finally, to calculate the error, we considered several different sources of uncertainty. First, the voltage box introduces a small error of $\sigma_{box} = 0.10$, according to the device manual provided at the JOS station. Second, the discrepancies in frequency readings introduce a relative error of

$$\begin{aligned} \sigma_f &= \frac{\left| f_{RF} - \frac{f_{CD}}{2} \right|}{f_{CD}} \\ &= \frac{\left| 9.5204 \text{ GHz} - \frac{19.130 \text{ GHz}}{2} \right|}{\frac{19.130 \text{ GHz}}{2}} \\ &\approx 0.0046628 \end{aligned}$$

where f_{RF} is the reading from the RF generator and f_{CD} is the reading from the crystal detector, divided by 2 to account for the doubling. I used f_{CD} as the "true" frequency value since the crystal detector provides a more reliable measurement. Lastly, the error from the voltage step is $\sigma_{step} = 0.06$, which I determined from the `CurveFit.m` script and represents the standard error between fitted and actual values. Altogether, the combined error is given by

$$\begin{aligned} \sigma_{K_J} &= \frac{2e}{h} \sqrt{\sigma_{box}^2 + \sigma_f^2 + \sigma_{step}} \\ &= (476.0 \text{ MHz}/\mu\text{V}) * \sqrt{(0.10)^2 + (0.0046628)^2 + (0.06)^2} \\ &\approx 56 \text{ MHz}/\mu\text{V} \end{aligned}$$

and the final result for the approximation of $\frac{2e}{h}$ is 476.0 ± 56 MHz/μV. This estimation is within error of the value of 483.5912 ± 0.0012 MHz/μV obtained by Parker, Taylor, and Langenberg [7]. However, we can attribute our greater value of error to having greater sources of uncertainty, particularly that of the voltage box.

6 Conclusion

Upon successful manipulation of the available parameters, my partner and I were able to observe the DC and AC Josephson effects both qualitatively and quantitatively. In analyzing the I-V characteristic in both DC and AC regimes, we gained valuable insight into the workings of the Josephson junction and ultimately produced a reliable estimate of the Josephson constant $\frac{2e}{h}$ to within error, obtaining a value of 476.0 ± 56 MHz/μV. As is good practice in scientific research, reproducing this famous experiment allowed us to check our own results against those of former groups and think critically about what sources of uncertainty could have contributed to any discrepancies. Performing the JOS experiment not only demystified the physics of superconductivity but also familiarized us with the safety protocols and procedural techniques involved in ultracold and condensed matter experiments.

7 Acknowledgements

I want to thank my partner Saavanth for filling in the frustrating silences with fun discussions of post-graduate plans and counting macronutrients for fitness. He does, in fact, lift.

Additionally, I want to acknowledge Christian Merino, Kelly Backes, and Katya Simpson, all of whom are current Physics 111B students who drew from their previous experiences with the JOS experiment to provide valuable advice and support.

References

[1] Clarke, John. (1970). The Josephson Effect and *e/h*. *American Journal of Physics*, 38(9), 1071-1093. doi: 10.1119/1.1976556

[2] "SQUID: The super-detector" Supraconductivite. Web. 6 Apr 2016. `http://www.supraconductivite.fr/en/index.php?p=applications-squid`

[3] "Josephson effect." Wikipedia. 23 Dec 2015. Web. 7 Apr 2016.

[4] "Cooper pair." Wikipedia. 17 Feb 2016. Web. 12 Apr 2016.

[5] Richard P. Feynman. "The Schroedinger Equation in a Classical Context: A Seminar on Superconductivity." *The Feynman Lectures on Physics, Vol. III: Quantum Mechanics*. New York, NY: Basic Books, 2011. Print.

[6] "Niobium." Wikipedia. 3 Apr 2016. Web. 12 Apr 2016.

[7] "JOS - Josephson Junction." Donald A. Glaser Advanced Experimentation Laboratory. Department of Physics, University of California, Berkeley. `http://experimentationlab.berkeley.edu/JOS`

[8] "Four Wire Measurement." Donald A. Glaser Advanced Experimentation Laboratory. Department of Physics, University of California, Berkeley. `http://physics111.lib.berkeley.edu/Physics111/Reprints/JOS/10-Four_Wire_Measurement.pdf`